Frequency-dependent bifurcation point between field-cooled and zero-field-cooled dielectric constant of $LiTaO_3$ nanoparticles embedded in amorphous SiO_2

Shigemi Kohiki,[a] Shintaro Kawakami, Shinichiro Nogami, Syozo Takada,[b] and Hirokazu Shimooka
Department of Materials Science, Kyushu Institute of Technology, Kitakyushu 804-8550, Japan

Masato Okui, Sei Fukushima, Masanori Mitome, and Yoshio Bando
Advanced Materials Laboratory, National Institute of Materials Science, Tsukuba, Ibaraki 305-0044, Japan

(Received 1 December 2003; accepted 26 February 2004)

Splitting between the field-cooled dielectric constant and the zero-field-cooled dielectric constant was observed for a diluted system of $LiTaO_3$ nanoparticles (diameter ≈30 Å) embedded in amorphous SiO_2. At the applied field frequency of 100 kHz, the real part of the field-cooled dielectric constant diverged from that of the zero-field-cooled one at ≈380 °C. The bifurcation point of the history-dependent dielectric constant rose from ≈310 to ≈540 °C upon increasing the field frequency from 10 to 1000 kHz. Bulk $LiTaO_3$ powders showed no splitting in the history-dependent dielectric constant and the maximum at 645 °C in the real part of the dielectric constant, despite the variation of frequency. Both the splitting of the history-dependent dielectric constant and the frequency dependence of the bifurcation point suggest that the $LiTaO_3$ nanoparticles with a single-domain structure were in the superparaelectric state as a consequence of insignificant cooperative interactions among the nanoparticles in the diluted system. The energy barrier of ≈0.9 eV separating two ($+p$ and $-p$) polarization states corroborated the potential of the $LiTaO_3$ nanoparticle for ultrahigh-density recording media applications. © *2004 American Institute of Physics.* [DOI: 10.1063/1.1715147]

Properties of nanominiaturized ferroelectric materials are of fundamental and technological interest.[1–6] Efforts to understand the physical properties of nanoparticles have been paralleled by attempts to exploit their beneficial properties. Nanoparticles with a long-lived remanent polarization are promising for development of low-power and nonvolatile memory devices that can be in operation above room temperature.

We have reported that the maximum temperature in the real part of temperature-dependent complex dielectric constants $T_m(\varepsilon')$ of $BaTiO_3$ (BTO), $SrBa_2Ta_2O_9$ (SBTO), and $LiTaO_3$ (LTO) nanoparticles embedded in amorphous SiO_2 were 60, 180, and 365 °C, respectively, at the applied field frequency (f) of 100 kHz.[7–10] The ferroelectric–paraelectric transition temperatures $T_c(\varepsilon')$ of the bulk BTO, SBTO, and LTO, powders were 130, 310, and 645 °C, respectively. For BTO, SBTO, LTO, the T_m values were lower than the T_c values by 70, 130, and 280 °C, respectively. The nanominiaturization of the ferroelectric materials brought about larger lowering of the characteristic temperature for the material with higher T_c. With the increase of f from 10 to 1000 kHz, the maximum temperature in the imaginary part of temperature-dependent complex dielectric constant $T_m(\varepsilon'')$ for the diluted system of LTO nanoparticles rose from 285 to 420 °C.[10] Despite the variation of f, $T_c(\varepsilon'')$ of the bulk LTO powders remained at 615 °C. A rise of T_m with increasing f is similar to that reported for dipolar glasses,[11] and is an indication of slow relaxation processes that characterize the glassy behavior.[12]

Ferroelectric nanoparticles smaller than the ferroelectric domain size have a single-domain structure.[10,13] In addition, there is no long-range ferroelectric order in a diluted system of the nanoparticles. All energies as a function of polarization for nanoparticles with insignificant cooperative interactions depend on their size, thus, the energy barrier separating alternative polarization states ($+p$ and $-p$) of the nanoparticle decreases as the size decreases, and the polarization state of the nanoparticle becomes unstable against thermal agitation. As a consequence of random distribution of the polarization direction of individual nanoparticles, the system is in the superparaelectric state below T_c and exhibits paraelectriclike behavior above T_m. The dipole moment of each nanoparticle disappears at T_c and the system reaches intrinsic paraelectric state.[7–10] In diluted systems of ferroelectric nanoparticles, the local ordering is due to electric dipoles. The spin representing a magnetic moment of magnetic spin glasses turns into a pseudospin representing the electric moment of dipolar glasses. Here, we treat the dielectric constant instead of magnetic susceptibility, otherwise, the situation for diluted systems of ferroelectric nanoparticles is similar to that for magnetic spin glasses. A spin glass is modeled as a system of interacting superparamagnetic particles.[11] The shift of T_m with f for superparamagnets is much larger than that for spin glasses.[12] For the diluted sys-

[a]Electronic mail: kohiki@che.kyutech.ac.jp
[b]Permanent address: Advanced Semiconductor Research Center, National Institute of Advanced Industrial Science and Technology, Tsukuba, Ibaraki 305-8569, Japan.

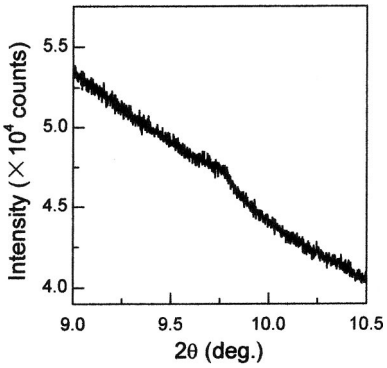

FIG. 1. Synchrotron radiation x-ray diffraction pattern of the diluted system of LTO nanoparticles embedded in the amorphous SiO_2 matrix.

tem of LTO nanoparticles, the relative variation of T_m per decade of f, $(\Delta T_m/T_m)/\Delta(\log_{10} f) \approx 0.1$, indicates that the system was in the superparaelectric state.[10,12]

It is well known that the response of the glassy system to an external field depends on the history of the system. Specifically, if the system has been cooled in an external field, the corresponding field-cooled (FC) dielectric constant $\varepsilon_{FC}(T)$ will differ from the zero-field-cooled (ZFC) one $\varepsilon_{ZFC}(T)$, which is observed after cooling the sample in zero field. As the temperature lowers, $\varepsilon_{FC}(T)$ and $\varepsilon_{ZFC}(T)$ curves diverge from each other at the bifurcation point (T_{bif}). $\varepsilon_{ZFC}(T)$ then deviates below $\varepsilon_{FC}(T)$, and shows a maximum at T_m corresponding to the freezing temperature of the glassy system. An Arrhenius-type behavior of relaxation times produces a slowing-down of the motions of the dipole moment, even above T_m. A shift of T_{bif} with f is a clear indication of the glassy nature of dipolar glasses. Splitting between $\varepsilon_{FC}(T)$ and $\varepsilon_{ZFC}(T)$ has been observed in many glassy systems.[11] However, there has been no report on the splitting of $\varepsilon_{FC}(T)$ and $\varepsilon_{ZFC}(T)$, nor on the frequency dependence of T_{bif} for the diluted ferroelectric nanoparticles. For a diluted system of LTO nanoparticles ($\phi \approx 30$ Å), we confirmed both splitting between $\varepsilon_{FC}(T)$ and $\varepsilon_{ZFC}(T)$ and a rise of T_{bif} with increasing f.

Since the spontaneous polarization of LTO crystals is so large (50 $\mu C/cm^2$),[14,15] the LTO nanoparticle is promising for ultrahigh-density memory device applications. For fabrication of the diluted system of LTO nanoparticles, we used the mesopores of the MCM-41 molecular sieve[16] as a growth template of the nanoparticles. The MCM-41 was soaked in 0.01 mol/l absolute ethanol solution of lithium chloride and tantalum chloride, and then calcined at 850 °C. The concentration of LTO determined by energy-dispersive x-ray analysis was approximately 0.8 mol %. We found barely an indication of the formation of LTO nanoparticles, even in the x-ray diffraction measurement using synchrotron radiation ($\lambda = 0.636$ Å) at the BL15XU of SPring-8, Japan. A smeared and rather broad hump was observed at the diffraction angle ($2\theta \approx 9.75°$) corresponding to the LTO (012) reflection (JCPDS No. 29-0836), as shown in Fig. 1. However, it is hard to manifest the formation of nanoparticles since the hump is buried in an intense background due to the diffuse scattering of amorphous SiO_2. The signal-to-noise ratio was almost equal to or less than 2. A transmission electron microscope (TEM) was used to examine directly the formation

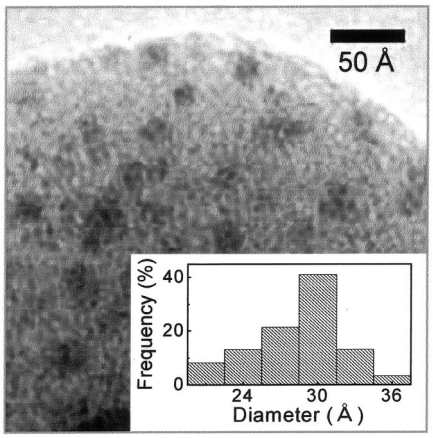

FIG. 2. A representative TEM image of the LTO nanoparticles dispersed in the matrix. Inset: Particle size distribution deduced from the image of 600 $\times 600$ Å^2 region.

of LTO nanoparticles.[17] As shown by the dark spots in the bright-field image of Fig. 2, the particles were distributed randomly in the matrix. The particles are well separated and no aggregation occurred. The average size of the particles was ≈30 Å, as shown by the inset of Fig. 2. The particles are monodisperse with $\sigma \leqslant 5\%$ in diameter. The Li K energy-loss spectrum and Ta L and M x-ray spectra measured by the TEM confirmed that the dark spots correspond to the LTO nanoparticles dispersed in SiO_2.

In order to confirm the glassy nature of the diluted LTO nanoparticles, we examined history dependence of $\varepsilon^*(f,T) = \varepsilon' + i\varepsilon''$ at temperatures T from 200 to 750 °C with f from 10 to 1000 kHz.[18] Since the voltage applied to a sample 0.5 mm thick was 10 V, the probing field E_{ac} was 0.2 kV/cm, smaller than the coercive field E_c (160 kV/cm) of LTO.[14,15] Figure 3 shows the temperature dependence of ε'_{FC} and ε'_{ZFC} from 200 to 600 °C at f of 10, 50, 100, 500, and 1000 kHz of the diluted system of LTO nanoparticles embedded in the SiO_2 matrix. The splitting between ε'_{FC} and ε'_{ZFC} has indeed been observed at each f. Similar to what we have already reported,[10] the matrix showed gradually increasing ε' with T

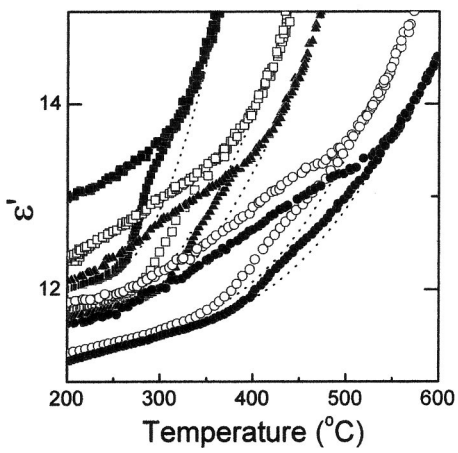

FIG. 3. Temperature dependence of history-dependent dielectric constant from 200 to 600 °C at f of 10 (■), 50 (□), 100 (▲), 500 (○), and 1000 kHz (●) of the diluted system of LTO nanoparticles embedded in the matrix. At each f, upper and lower arms of the bifurcation correspond to ε'_{FC} and ε'_{ZFC}, respectively. The dotted line for each f represents background in $\varepsilon'(T)$ due to ionic conduction increasing with T.

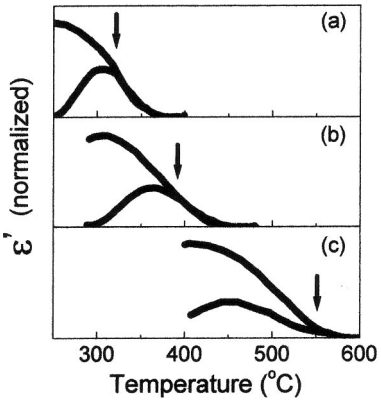

FIG. 4. Background subtracted and normalized ε'_{FC} (upper arm) and ε'_{ZFC} (lower arm) at around the bifurcation point of the LTO nanoparticles at f of 10 (a), 100 (b), and 1000 (c) kHz. Arrows correspond to the bifurcation points.

at each f. The bulk LTO powders showed the peak in $\varepsilon'(T)$ at 645 °C, regardless of the variation in f. We found no splitting in the history-dependent dielectric constant of either the matrix or the bulk LTO powders below 750 °C. Therefore, the observed splitting between ε'_{FC} and ε'_{ZFC} for the diluted system of LTO nanoparticles can be attributed to the nanominiaturized ferroelectric materials. We assumed that the background in $\varepsilon'(T)$ presented by the dotted line for each f in Fig. 3 was formed by ionic conduction increasing with T. Figure 4 shows the background subtracted and normalized ε'_{FC} and ε'_{ZFC} for the nanoparticles at f of 10, 100, and 1000 kHz. The relative variation of $T_m(\varepsilon'_{ZFC})$ per decade of f was ≈ 0.1, which indicates that the LTO nanoparticles were in the superparaelectric state.[12] The temperature at which the splitting between ε'_{FC} and ε'_{ZFC} should occur shifted pronouncedly to the higher temperature side with increasing f. The shift of T_{bif} with f represents strong evidence of the glassy nature for the diluted system of LTO nanoparticles, as mentioned before.

Progressive freezing of the motions of the dipole moment of the LTO nanoparticles began immediately below T_{bif}. Two polarization states, $+p$ and $-p$, in a superparaelectric potential having double minima are separated by an energy barrier U, which is approximately equal to the product of the Gibbs free energy density and the nanoparticle volume. The freezing appears through the probability of each nanoparticle to overcome U, and is expressed in terms of relaxation time $\tau = \tau_0 \exp(U/k_B T)$, where $\tau = 1/f$ is the measuring time, τ_0 is the characteristic relaxation time, and k_B is the Boltzmann constant. On lowering the temperature, the relaxation time increases and a peak in $\varepsilon'_{ZFC}(T)$ will appear at the freezing temperature T_f, when τ becomes larger than τ_0. While the observed T_m is not a true static quantity, we have estimated the U value in order to evaluate the dielectric stability of individual LTO nanoparticle. T_m at f of 10, 50, 100, 500, and 1000 kHz were 305, 332, 363, 437, and 457 °C, respectively. By using T_m as T_f in the equation $T_f = U/k_B \ln(1/\tau_0 f)$, with $\tau_0 = 1 \times 10^{-12}$ s,[10,19] we obtained the U/k_B values of approximately 0.908, 0.885, 0.883, 0.878, and 0.869 eV at f of 10, 50, 100, 500, and 1000 kHz, respectively. The rise in T lessened the Gibbs free energy density of the nanoparticle, however, the U/k_B value of ≈ 0.9 eV implies that the dielectric stability of the LTO nanoparticle is sufficient for nonvolatile memory devices to be in operation above room temperature.

For the diluted system of LTO nanoparticles embedded in SiO_2, we have observed the splitting between ε'_{FC} and ε'_{ZFC} below T_c of the bulk $LiTaO_3$ and the rise of T_{bif} with increasing f. Such frequency dependence confirms the superparaelectric nature of the LTO nanoparticles dispersed in the matrix. The dielectric stability sufficient for potential ferroelectric-memory applications was observed for the LTO nanoparticle.

One of the authors (S.K.) thanks the support from the Murata Science Foundation for this work. A part of this work was supported by "Nanotechnology Support Project" of the Ministry of Education, Culture, Sports, Science and Technology (MEXT), Japan.

[1] D. McCauley, R. E. Newnham, and C. A. Randall, J. Am. Ceram. Soc. **81**, 979 (1998).
[2] A. Shaikh, R. Vest, and G. Vest, IEEE Trans. Ultrason. Ferroelectr. Freq. Control **36**, 407 (1990).
[3] S. Schlag and H. F. Eicke, Langmuir **10**, 3357 (1994).
[4] J. U. Muller and K. Barner, Ferroelectrics **108**, 83 (1990).
[5] M. Anliker H. R. Brugger, and T. Kanzig, Helv. Phys. Acta **27**, 99 (1954).
[6] K. Uchino, E. Sadanaga, and T. Hirose, J. Am. Ceram. Soc. **72**, 1555 (1989).
[7] S. Kohiki, S. Takada, A. Shimizu, K. Yamada, and H. Higashijima, J. Appl. Phys. **87**, 474 (2000).
[8] S. Kohiki, S. Takada, A. Shimizu, K. Yamada, and H. Higashijima, J. Appl. Phys. **88**, 6093 (2000).
[9] H. Higashijima, S. Kohiki, S. Takada, A. Shimizu, and K. Yamada, Appl. Phys. Lett. **75**, 3189 (1999).
[10] S. Kohiki, S. Nogami, S. Kawakami, S. Takada, H. Shimooka, H. Deguchi, M. Mitome, and M. Oku, Appl. Phys. Lett. **82**, 4134 (2003).
[11] K. Binder and A. P. Young, Rev. Mod. Phys. **58**, 801 (1986).
[12] J. A. Mydosh, *Spin Glasses: An Experimental Introduction* (Taylor & Francis, London, 1993).
[13] L. E. Cross, Ferroelectrics **76**, 241 (1987).
[14] Landolt-Börnstein, *Numerical Data and Functional Relationships in Science and Technology*, New Series Vol. 16, edited K. H. Hellwege and A. M. Hellwege (Springer, Berlin, 1981), p. 157.
[15] V. Gopalan and M. C. Gupta, Appl. Phys. Lett. **68**, 888 (1996).
[16] For example, C. T. Kresge, M. E. Leonowicz, W. J. Roth, J. C. Vartuli, and J. S. Beck, Nature (London) **359**, 710 (1992).
[17] A JEOL JEM-3100FEF was used for TEM analysis. See M. Mitome, Y. Bando, D. Golberg, K. Kurushima, Y. Okura, T. Kaneyama, M. Naruse, and Y. Honda, Microsc. Res. Tech. **63**, 140 (2004).
[18] An HP4291 RF impedance analyzer was employed for the measurement. Since the signal of the nonlinear dielectric response was so weak, we could not clarify the absence of cusp in the third-harmonic component of $\varepsilon^*(f,T)$.
[19] A. Levstik, Z. Kutnjak, C. Filipič, and R. Pirc, Phys. Rev. B **57**, 11204 (1998).